

A Statistical Framework for Model Selection in LSTM Networks

Fahad Mostafa ^{*1}

¹School of Mathematical and Natural Sciences, Arizona State University, USA

Abstract

Long Short-Term Memory (LSTM) neural network models have become the cornerstone for sequential data modeling in numerous applications, ranging from natural language processing to time series forecasting. Despite their success, the problem of model selection, including hyperparameter tuning, architecture specification, and regularization choice remains largely heuristic and computationally expensive. In this paper, we propose a unified statistical framework for systematic model selection in LSTM networks. Our framework extends classical model selection ideas, such as information criteria and shrinkage estimation, to sequential neural networks. We define penalized likelihoods adapted to temporal structures, propose a generalized threshold approach for hidden state dynamics, and provide efficient estimation strategies using variational Bayes and approximate marginal likelihood methods. Several biomedical data centric examples demonstrate the flexibility and improved performance of the proposed framework.

Keywords LSTM; model selection; penalized likelihood; variational Bayes; shrinkage estimation; information criterion

AMS Classification 62M10; 92B20; 62P10; 62P99

1 Introduction

Forecasting is a fundamental analytical process that involves estimating future outcomes based on historical and current data patterns. Among various forecasting approaches, time series forecasting focuses on sequential data indexed over time and has proven indispensable for capturing temporal dependencies and trends. This type of forecasting plays a crucial role in decision-making across numerous fields, ranging from short-term predictions to long-term strategic planning. In the era of artificial intelligence, the advancements in data acquisition and computational methods have further amplified the importance of reliable neural network-based forecasting. In healthcare, accurate time series predictions support clinical decision-making and patient monitoring (Forkan and Khalil (2017)). In meteorology, predictive models aid in early warning systems and climate modeling (Chantry et al. (2021)). Similarly, time series methods are integral in analyzing physiological signals such as ECG and EEG for early anomaly detection (Andrysiak (2016); Wang et al. (2016)), optimizing energy usage and load forecasting in smart grids (Muralitharan et al. (2018)), and modeling complex economic indicators in econometrics (Moshiri and Cameron (2000); Kuan and White (1994)).

Clinical time series forecasting is an essential task in modern healthcare, enabling proactive decision-making by predicting future physiological states or clinical outcomes based on temporally ordered medical data (Morid et al. (2023)). Electronic Health Records (EHRs), vital signs, lab results, and wearable sensor data offer a wealth of time-stamped information that can be leveraged to anticipate disease progression, detect early warning signs, and optimize resource allocation (Andrysiak (2016); Wang et al. (2016); Ray et al. (2020)).

However, clinical time series data are inherently complex, characterized by irregular sampling, missing values, varying sequence lengths, and strong nonlinear dependencies. Traditional statistical models often fall short in capturing these intricacies. In response, artificial intelligence (AI) and machine learning (ML)

^{*}Corresponding author: Fahad Mostafa Email: fahad.mostafa@asu.edu

techniques have emerged as powerful tools for modeling such data, offering the capacity to learn rich representations and temporal dynamics without manual feature engineering or model selection, see in (Khurana et al. (2018)). Given its wide applicability, developing robust and generalizable forecasting models remains a central research challenge, especially in the presence of noisy, nonlinear, or multivariate time series data.

Model selection is a fundamental challenge in statistical modelling and machine learning. In classical settings, techniques such as stepwise regression ((Miller, 2002)), information criteria like AIC ((Akaike, 1974)) and BIC ((Schwarz, 1978)), and penalized likelihood methods including LASSO ((Tibshirani, 1996)) are standard tools. In the context of neural networks, early contributions attempted to frame them within statistical inference frameworks ((White, 1989; Ripley, 1993)), although widespread adoption emphasized predictive performance over parsimony.

Feedforward neural networks (FNNs) have been historically viewed as flexible approximators ((Hornik et al., 1989)), but lacked statistically grounded model selection procedures. Recent work has introduced information-criteria-based selection for FNNs ((McInerney and Burke, 2024)), providing principled alternatives to brute-force hyperparameter tuning. Others have explored criteria for pruning ((LeCun et al., 1990)) or automatic architecture selection using sparsity-inducing priors ((Sun et al., 2022)).

In the recurrent setting, model selection for LSTM networks has largely relied on grid search and validation loss ((Greff et al., 2017; Fischer and Krauss, 2018)). However, this often leads to overparameterization and poor interpretability. Bayesian LSTM variants ((Gal and Ghahramani, 2016; Fortunato et al., 2017)) introduce uncertainty-aware models, but do not address structured selection. Our approach builds on the recent trend of combining likelihood-based inference with neural architectures ((Tran et al., 2020)), adapting it for LSTM networks through a statistically grounded, BIC-driven model selection framework.

While LSTM networks have become a dominant approach for modeling sequential and time-dependent data, particularly in clinical forecasting tasks, their use is often driven by predictive performance rather than statistical rigor (Yu et al. (2019)). LSTM models, like many deep learning architectures, are typically treated as black-box systems with high capacity and numerous tunable hyperparameters, such as the number of layers, units, and dropout rates. This emphasis on prediction over parsimony often leads to over-parameterized and potentially unstable models (Greff et al. (2016)). In contrast, traditional statistical modeling emphasizes model selection as a means of balancing fit and complexity to ensure interpretability, generalizability, and robust inference (Efron (2012)). However, despite their complexity, LSTMs can be integrated into a more statistically grounded framework through simulation-based validation, the application of penalized likelihood methods, and information-theoretic model selection criteria such as Akaike Information Criterion (AIC), and Bayesian Information Criterion (BIC) (Chakrabarti and Ghosh (2011)). Bridging this gap between machine learning and statistical methodology is crucial for increasing the utility and trustworthiness of LSTM models, especially in high-stakes domains like clinical decision support. The LSTM network, introduced by Hochreiter and Schmidhuber (1997), is a special type of recurrent neural network capable of learning long-term dependencies in sequential data (Schmidhuber (2022)). LSTMs have been successfully applied in fields as diverse as language modelling (De Mulder et al. (2015)), speech recognition (Sundermeyer et al. (2015)), and financial time series forecasting (Cao et al. (2019)). Despite their empirical success, LSTM networks face two critical challenges: overfitting and architecture specification. Despite the widespread use of LSTM models in various applications (Dog˘an (2020); Moshiri and Cameron (2000); Yu et al. (2019); Cao et al. (2019)), there is a lack of statistically robust methodologies, including model selection procedures, simulation-based validation studies, and evaluations of computational performance. Unlike classical models where the number of parameters is relatively small, LSTMs involve a large number of weights distributed across gates, cells, and hidden states. At each time step, the LSTM receives both the current value of the target variable and the corresponding values of the covariates, enabling the model to learn complex temporal dependencies while conditioning its predictions on influential external information. This multi-input structure helps improve forecasting accuracy, especially when the target series is affected by factors beyond its own history. Hence, model selection, that is, the systematic choice of model complexity via variable selection, and regularization, is pivotal for achieving good generalization performance. In classical statistical models, tools like AIC, BIC, and shrinkage methods such as LASSO provide principled model selection mechanisms (Chakrabarti and Ghosh (2011)). Extending these ideas to LSTMs is nontrivial due to their nonlinearity, sequential dependence, and high-dimensional parameter spaces.

This paper proposes a unified framework to bridge this gap by: (i) formulating penalized likelihood criteria for sequential data models; (ii) adapting shrinkage methods to the internal structure of LSTMs; (iii)

introducing temporal information criteria; and (iv) developing computational strategies for estimation. We begin by reviewing the LSTM architecture in Section 2, followed by a discussion of model selection theory in Section 3. Section 4 presents estimation techniques, Section 5 provides illustrative examples, and Section 6 concludes the paper by brief discussions.

2 Long Short-Term Memory Networks: A Statistical Perspective

2.1 LSTM Model Formulation

The LSTM network is a type of recurrent neural network designed to overcome the vanishing gradient problem and enable learning over long temporal sequences, e.g. (Sherstinsky (2020); Zhao et al. (2017); Cao et al. (2019)). It achieves this through a gated cell structure that regulates the flow of information. Consider a sequence of inputs $\{x_t\}_{t=1}^T$. At each time step t , an LSTM cell updates its internal cell state c_t and produces a hidden state h_t based on the current input x_t , the previous hidden state h_{t-1} , and the previous cell state c_{t-1} . The update mechanism involves three types of gates: the input gate, forget gate, and output gate, defined as follows:

$$\begin{aligned}
i_t &= \sigma(W_i x_t + U_i h_{t-1} + b_i), & (\text{input gate}) \\
f_t &= \sigma(W_f x_t + U_f h_{t-1} + b_f), & (\text{forget gate}) \\
o_t &= \sigma(W_o x_t + U_o h_{t-1} + b_o), & (\text{output gate}) \\
\tilde{c}_t &= \tanh(W_c x_t + U_c h_{t-1} + b_c), & (\text{candidate cell state}) \\
c_t &= f_t \odot c_{t-1} + i_t \odot \tilde{c}_t, & (\text{new cell state}) \\
h_t &= o_t \odot \tanh(c_t), & (\text{new hidden state})
\end{aligned} \tag{1}$$

Here, σ denotes the logistic sigmoid function, \tanh is the hyperbolic tangent activation function, and \odot represents elementwise multiplication. The matrices $W_{\{i,f,o,c\}}$ and $U_{\{i,f,o,c\}}$ are the input-to-hidden and hidden-to-hidden weight matrices, respectively, and $b_{\{i,f,o,c\}}$ are bias vectors. Each gate serves a distinct purpose: (i) Input gate i_t : Controls how much new information from the current input flows into the cell state. (ii) Forget gate f_t : Determines how much information from the previous cell state c_{t-1} is retained or forgotten. (iii) Output gate o_t : Controls the amount of cell state information exposed to the next hidden state h_t . The LSTM design enables the network to learn long-range dependencies by allowing gradients to flow unchanged through many time steps when the forget gate f_t is near 1 (see in Figure 1). The output y_t at each time step is typically a function of the hidden state:

$$y_t = \varphi(h_t; \theta), \tag{2}$$

where φ can be a simple linear mapping or a more complex nonlinear function parameterized by θ . In classification tasks, φ is often a softmax layer, while in regression tasks, it may be a linear projection. The capacity to regulate memory with dynamic gates makes LSTM networks highly effective for tasks involving sequential data in time series prediction, see in (Yu et al. (2019); Zhao et al. (2017); Sundermeyer et al. (2015)).

Figure 2 illustrates the structure-evolving process of a graph across five time steps, denoted as $G^{(0)}$ to $G^{(4)}$. Starting from an initial random graph $G^{(0)}$, the model iteratively merges a subset of node pairs to form higher-level abstract nodes, simulating the hierarchical representation learning mechanism in a structure-evolving LSTM. At each step, the red node represents the starting node, green nodes indicate its immediate neighbors, and black nodes are newly formed merged nodes. Arrows between successive graphs indicate the bottom-up evolution of the graph topology, where the node structure becomes increasingly coarser, allowing

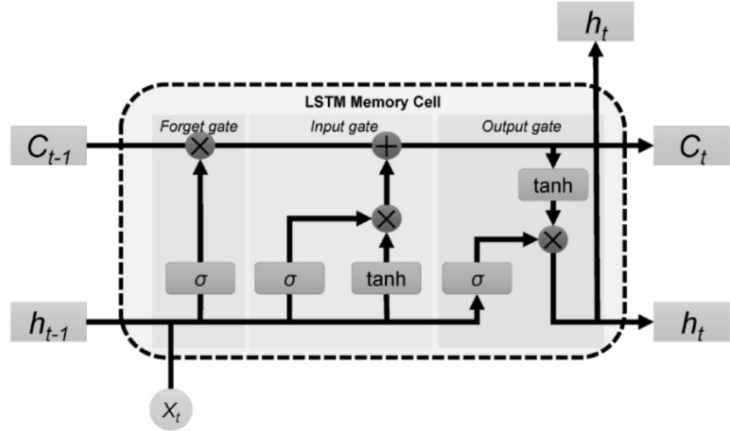


Figure 1: Architecture of an LSTM memory cell. The input x_t and the previous hidden state h_{t-1} are passed through three gates. The output gate uses the updated cell state to compute the new hidden state h_t , which serves as output and influences the next step. Sigmoid (σ) and tanh activations are used in various gates to control flow and scale.

information to be propagated through multi-scale representations. The arrows indicate sequential time steps of the graph transformation. This structure allows the LSTM to propagate information across different levels of graph abstraction, enabling effective spatio-temporal learning on non-Euclidean domains.

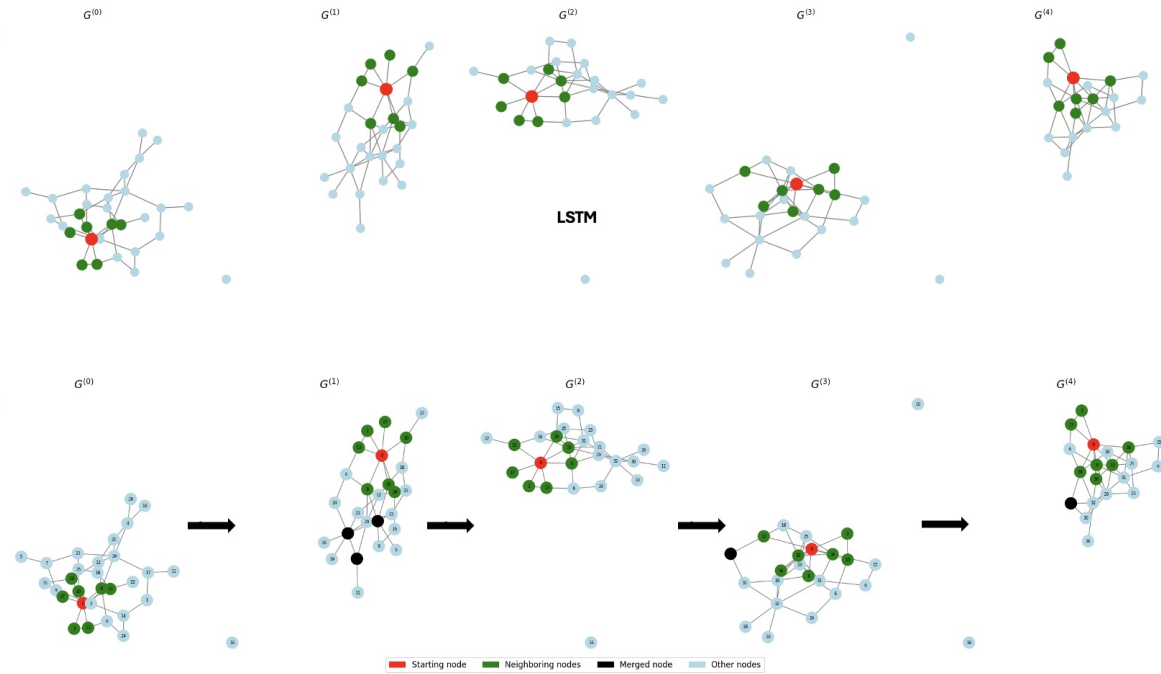


Figure 2: An illustration of the structure-evolving process in a graph-based LSTM model. The top row shows the original graph inputs $G^{(0)}$ through $G^{(4)}$ with node roles colored to indicate the starting node (red), its neighboring nodes (green), and all others (light blue). The bottom row further annotates merged nodes (black) and highlights how the hierarchical structure evolves over time via a bottom-up merging strategy.

2.2 Stochastic Interpretation

LSTM networks can be interpreted not only as deterministic mappings but also through a stochastic lens, emphasizing their structural analogy to latent variable models and state-space models. There are some recent works where researchers introduced stochastic connections of such deep neural networks (see Liu and Theodorou (2019); Song et al. (2018); Su et al. (2019)). Therefore for the LSTM model in section 2.1, let us consider a sequence of observations $\{y_t\}_{t=1}^T$ generated conditionally on hidden states $\{h_t\}_{t=1}^T$ and inputs $\{x_t\}_{t=1}^T$. The generative process for the LSTM can be framed as:

$$\begin{aligned} h_t &\sim p(h_t | h_{t-1}, x_t; \theta), \\ y_t &\sim p(y_t | h_t; \theta), \end{aligned}$$

where θ denotes all the network parameters including weights and biases. Here, h_t represents a latent (unobserved) state that evolves over time, and y_t is the observed output at each time step. The hidden state transition $p(h_t | h_{t-1}, x_t; \theta)$ in the LSTM architecture is defined implicitly by the gating mechanisms and the update equations 1. Thus, h_t depends on h_{t-1} and x_t through a nonlinear, parameterized transformation governed by θ . Similarly, the emission distribution $p(y_t | h_t; \theta)$ models the generation of outputs. In many cases, this distribution is assumed to be Gaussian for continuous outputs or categorical for classification tasks:

$$y_t | h_t \sim \mathcal{N}(W_y h_t + b_y, \sigma^2 I) \quad (\text{continuous case})$$

$$y_t | h_t \sim \text{Categorical}(\text{softmax}(W_y h_t + b_y)) \quad (\text{classification case})$$

where W_y and b_y are the output layer parameters. The joint likelihood of the observations and hidden states is:

$$p(y_{1:T}, h_{1:T} | x_{1:T}; \theta) = \prod_{t=1}^T p(y_t | h_t; \theta) p(h_t | h_{t-1}, x_t; \theta). \quad (3)$$

In practice, inference involves marginalizing out the latent states $h_{1:T}$ to obtain the marginal likelihood:

$$p(y_{1:T} | x_{1:T}; \theta) = \int p(y_{1:T}, h_{1:T} | x_{1:T}; \theta) dh_{1:T}. \quad (4)$$

However, this integral is analytically intractable due to the complex nonlinearities of the LSTM dynamics in section 2.1. This motivates the use of approximate inference methods, such as variational inference, particle filtering, or Monte Carlo techniques. From a Bayesian viewpoint, one may place priors over the model parameters θ and hidden states h_t , treating LSTM as a hierarchical probabilistic model (see Yang et al. (2021)). Recent developments like Bayesian LSTMs extend this idea further by introducing posterior uncertainty over the parameters. Thus, the stochastic interpretation of LSTMs positions them within the rich framework of latent dynamic models, offering a principled foundation for uncertainty quantification, model selection, and regularization in sequential data modeling.

3 Proposed Model Selection in LSTM Networks

3.1 Penalized Likelihood Formulation

Model selection plays a crucial role in building efficient and generalizable Long Short-Term Memory models. Traditional model selection techniques, such as those based on maximum likelihood estimation (MLE) and information criteria (e.g., AIC, BIC), e.g. (Chaurasia and Harel (2013); Augustyniak (2014)), assume relatively simple model structures. However, LSTM networks involve large parameter spaces, complex temporal dependencies, and nonlinearities that render classical approaches insufficient (Yu et al. (2019)). To address these challenges, we propose a penalized likelihood framework specifically adapted to the characteristics

of LSTM architectures. Given a dataset $\{(x_t, y_t)\}_{t=1}^T$ consisting of input sequences x_t and corresponding outputs y_t , the standard objective in LSTM training is to maximize the log-likelihood:

$$\mathcal{L}(\theta) = \sum_{t=1}^T \log p(y_t | h_t(\theta)), \quad (5)$$

where $h_t(\theta)$ denotes the hidden state at time t , implicitly determined by the model parameters θ . The likelihood captures how well the model explains the observed data but does not penalize model complexity, potentially leading to overfitting, especially when networks are deep and wide, e.g. (Baek and Kim (2018); Medeiros et al. (2006); Connor et al. (1994)). To counteract overfitting, a penalization term $\Omega(\theta)$ is introduced based on several common penalization techniques, e.g. (Evgeniou et al. (2002); Bickel et al. (2006)), resulting in the penalized likelihood objective:

$$\mathcal{L}_p(\theta) = \sum_{t=1}^T \log p(y_t | h_t(\theta)) - \lambda \Omega(\theta), \quad (6)$$

where $\lambda > 0$ is a regularization parameter controlling the trade-off between model fit and complexity. The choice of penalty $\Omega(\theta)$ is critical. Several options are available.

(i) L2 Regularization (Ridge Penalty): Penalizes the squared ℓ_2 -norm of the weights, leading to shrinkage but not sparsity. Particularly useful for stabilizing weight magnitudes:

$$\Omega(\theta) = \sum_{g \in \{i, f, o, c\}} (\|W_g\|_2^2 + \|U_g\|_2^2). \quad (7)$$

(ii) L1 Regularization (Lasso Penalty): Penalizes the ℓ_1 -norm of the weights, encouraging sparsity and automatic feature selection:

$$\Omega(\theta) = \sum_{g \in \{i, f, o, c\}} (\|W_g\|_1 + \|U_g\|_1). \quad (8)$$

(iii) Group Lasso Penalty: Given the structured nature of LSTM parameters (grouped into gates and hidden-to-hidden connections), group sparsity can be enforced by using group lasso:

$$\Omega(\theta) = \sum_{g \in \{i, f, o, c\}} \left(\sqrt{d_g} \|W_g\|_2 + \sqrt{d_g} \|U_g\|_2 \right), \quad (9)$$

where W_g are the input-to-gate weights, U_g are the hidden-to-gate recurrent weights, d_g denotes the dimensionality of group g . Each type of penalty reflects different assumptions about model complexity and desired inductive biases. For instance, ℓ_1 -penalties are preferable when expecting that only a few gates or connections are important, whereas ℓ_2 -penalties are useful for smooth, well-behaved parameterizations. Beyond classical penalties, more advanced forms tailored to recurrent structures can be considered (Wu et al. (2021); Capliez et al. (2023)), such as: (i) Temporal Dropout Penalties: Randomly dropping connections across time steps, thus imposing temporal sparsity. (ii) Path Norm Regularization: Controlling the norm of the paths through the network, rather than individual weights. Choosing the regularization strength λ is another key consideration in many articles (Bischl et al. (2023)). Cross-validation over sequential splits or more sophisticated Bayesian optimization methods are utilized to adaptively determine λ . In addition, the penalized likelihood framework naturally connects to Bayesian interpretations. For example, an ℓ_2 -penalty corresponds to assuming Gaussian priors over parameters, while an ℓ_1 -penalty corresponds to Laplace priors. This duality provides a probabilistic underpinning for regularization and opens avenues for full Bayesian model selection approaches in LSTM networks. In summary, penalized likelihood methods provide a principled and flexible foundation for model selection in LSTM architectures. By carefully choosing the form of $\Omega(\theta)$ in equations (7), (8), (9), as well as optimizing the penalized objective, it is possible to balance predictive performance and generalization, ultimately leading to more reliable and interpretable sequential models.

3.2 Shrinkage on Gates and Hidden States

In traditional statistical models, shrinkage methods such as ridge regression or LASSO are employed to prevent overfitting and perform variable selection (Evgeniou et al. (2002); Hastie et al. (2009)). Inspired by these ideas, we propose applying structured shrinkage techniques to specific components of the LSTM architecture, namely the gates and hidden states. From the section 2.1, the LSTM cell involves the following gates: the input gate i_t , forget gate f_t , output gate o_t , and candidate cell update g_t (sometimes also referred to as the cell input modulation gate). We assign, each gate with its associated parameters:

$$(W_g, U_g, b_g), \quad g \in \{i, f, o, c\}.$$

where W_g are the input-to-gate weights, U_g are the hidden-to-gate recurrent weights, and b_g are the biases. To encourage sparsity and improve generalization, we propose the following structured penalization:

$$\Omega(\theta) = \sum_{g \in \{i, f, o, c\}} (\alpha_1 \|W_g\|_1 + \alpha_2 \|U_g\|_1) + \alpha_3 \|b_g\|_1, \quad (10)$$

where $\alpha_1, \alpha_2, \alpha_3 \geq 0$ are hyperparameters controlling the strength of shrinkage on the different parameter groups. Shrinkage on W_g promotes input feature selection, determining which external inputs are most influential for a specific gate. Shrinkage on U_g encourages sparsity in the recurrent connections, controlling memory dynamics over time. Shrinkage on b_g ensures that biases do not lead to unbalanced gate activations without strong evidence. Additionally, regularization is introduced directly at the hidden state level. This is achieved through techniques like *variational dropout* or *recurrent zoneout*, which impose noise or structured sparsity on hidden units:

$$h_t \sim \text{Dropout}(h_t; p), \quad (11)$$

where p denotes the dropout probability. An alternative explicit shrinkage formulation on hidden states is:

$$\Omega_{\text{hidden}}(\theta) = \beta \sum_{t=1}^T \|h_t\|_1, \quad (12)$$

where $\beta > 0$ controls the amount of sparsity enforced on the hidden activations across time. There are benefits of Structured Shrinkage, such as (i) Feature Selection: Identify the most relevant inputs contributing to long-term memory formation. (ii) Gate Simplification: Reduce model complexity by pruning unnecessary or redundant gate computations. (iii) Temporal Regularization: Stabilize hidden states over long sequences, improving robustness. (iv) Interpretability: Provide insights into the dynamics and decision processes learned by the LSTM. Such structured penalties can be seamlessly integrated into the overall learning objective by minimizing the penalized negative log-likelihood:

$$\mathcal{L}(\theta) = -\log p(y_{1:T} | x_{1:T}; \theta) + \lambda \Omega(\theta) + \lambda_{\text{hidden}} \Omega_{\text{hidden}}(\theta), \quad (13)$$

where $\lambda, \lambda_{\text{hidden}} \geq 0$ are tuning parameters controlling the strength of the regularization terms. Choosing the optimal regularization parameters can itself be part of the model selection process, using techniques such as cross-validation, Bayesian optimization, or information criteria adapted for sequential data. We propose gate-specific penalties from equation (8):

$$\Omega(\theta) = \sum_{g \in \{i, f, o, c\}} (\alpha_1 \|W_g\|_1 + \alpha_2 \|U_g\|_1).$$

Shrinkage on hidden states can be introduced via variational dropout (Nalisnick et al. (2019); Nguyen et al. (2021)). Selecting an appropriate LSTM model architecture is crucial to balance model complexity and generalization ability. Overly complex models risk overfitting, while overly simple models may underfit the data. Classical model selection criteria, such as AIC and BIC (Chakrabarti and Ghosh (2011), Akaike (1974)), provide statistically grounded methods for evaluating model fit while penalizing complexity. However, adapting these criteria to LSTM networks requires accounting for the sequential and high-dimensional nature of the data, as well as the stochastic dependence across time steps.

3.3 Information Criteria for Sequential Models

From the proposed model selection in section 3, the LSTM model with parameters θ , the log-likelihood of the observed sequence $y_{1:T}$ conditioned on the input sequence $x_{1:T}$ is denoted by: $\ell(\theta) = \log p(y_{1:T} | x_{1:T}; \theta)$. The classical AIC and BIC can be extended to sequential models as:

$$\text{AIC}_T = -2\ell(\hat{\theta}) + 2 \text{df},$$

$$\text{BIC}_T = -2\ell(\hat{\theta}) + \log(T) \text{df},$$

where: $\hat{\theta}$ is the maximum likelihood or penalized likelihood estimate of the model parameters, df (degrees of freedom) represents the effective number of free parameters, T is the total number of observed time points. The degrees of freedom: df in an LSTM model that include: (a) All weight matrices and biases in the input, forget, output, and candidate gates, (b) Output layer parameters, (c) Additional regularization parameters if applicable. In high-dimensional settings, it is more appropriate to estimate df based on the number of non-zero parameters, particularly if sparsity-inducing regularization (e.g., ℓ_1 -penalty) is applied. The term $-2\ell(\hat{\theta})$ measures the goodness of fit. Higher likelihood (less negative value) implies better fit. The penalty term (either 2df or $\log(T) \text{df}$) discourages overfitting by penalizing more complex models. AIC tends to favor more complex models compared to BIC, as $\log(T) > 2$ for typical sequence lengths.

4 Estimation Techniques

Training LSTM models within the statistical framework proposed in section 3 requires careful handling of hidden states and latent variables. Direct maximization of the marginal likelihood is generally intractable due to the complex, nonlinear, and recursive dependence of hidden states across time. In this section, we discuss two main strategies for approximate estimation: variational inference and adaptive Gauss-Hermite quadrature. There are many examples of these popular methods that are found in (Tran et al. (2017); Šmídl and Quinn (2006); Jin and Andersson (2020))

4.1 Variational Inference

To deal with the intractability of integrating over the hidden states, we propose the use of variational Bayes methods like the recent developments (see Šmídl and Quinn (2006)). Variational inference approximates the true posterior distribution $p(h_{1:T} | y_{1:T}, x_{1:T}; \theta)$ with a tractable variational distribution $q(h_{1:T})$ that is optimized to be as close as possible to the true posterior. The evidence lower bound (ELBO) on the log marginal likelihood is given by:

$$\log p(y_{1:T}) \geq \mathbb{E}_{q(h_{1:T})} [\log p(y_{1:T}, h_{1:T}) - \log q(h_{1:T})]. \quad (14)$$

Maximizing the ELBO with respect to both the model parameters θ and the variational parameters allows approximate inference while optimizing the predictive performance of the model. A key practical innovation for efficient optimization is the use of the reparameterization trick. Instead of directly sampling from $q(h_{1:T})$, we express $h_{1:T}$ as a deterministic function of a parameter and a noise variable, enabling low-variance gradient estimates of the ELBO via standard backpropagation methods. Specifically, if we assume $q(h_t) = \mathcal{N}(\mu_t, \sigma_t^2)$, then samples can be generated as:

$$h_t = \mu_t + \sigma_t \epsilon_t, \quad \epsilon_t \sim \mathcal{N}(0, 1).$$

This reparameterization enables gradients with respect to μ_t and σ_t to be computed efficiently, making the approach scalable to large datasets and long sequences. Furthermore, amortized variational inference can be used, where the variational parameters (μ_t, σ_t) are outputs of an inference network conditioned on the inputs x_t , reducing the number of free parameters and improving generalization.

4.2 Adaptive Gauss-Hermite Quadrature

For smaller models or situations where more accurate approximations of the marginal likelihood are needed, we propose the use of adaptive Gauss-Hermite quadrature (AGHQ), just like (Jin and Andersson (2020)). In our context, AGHQ adapts the quadrature nodes based on the posterior mode and local curvature (Hessian) of the log-posterior distribution of the hidden states. Specifically, the integral over h_t is centered at the mode \hat{h}_t and scaled according to the local covariance structure, resulting in improved approximation accuracy even with relatively few quadrature points. The procedure involves the following steps:

- Compute the posterior mode \hat{h}_t by maximizing $\log p(h_t | y_t, x_t; \theta)$.
- Approximate the local curvature via the second derivative (Hessian) at \hat{h}_t .
- Transform the standard quadrature nodes accordingly.

Adaptive quadrature is particularly useful when hidden state distributions are close to Gaussian but slightly skewed or heavy-tailed, as often happens with complex LSTM dynamics. Although AGHQ is computationally more intensive than variational inference, it provides highly accurate approximations for models with a moderate number of latent variables, making it ideal for offline applications or where interpretability and precise uncertainty quantification are important. In summary, variational inference provides a scalable and flexible method suitable for large-scale LSTM models, while adaptive quadrature offers a precise alternative for smaller, more interpretable models. The choice between these methods can be guided by the trade-off between computational resources and desired approximation accuracy (see Stringer (2021)).

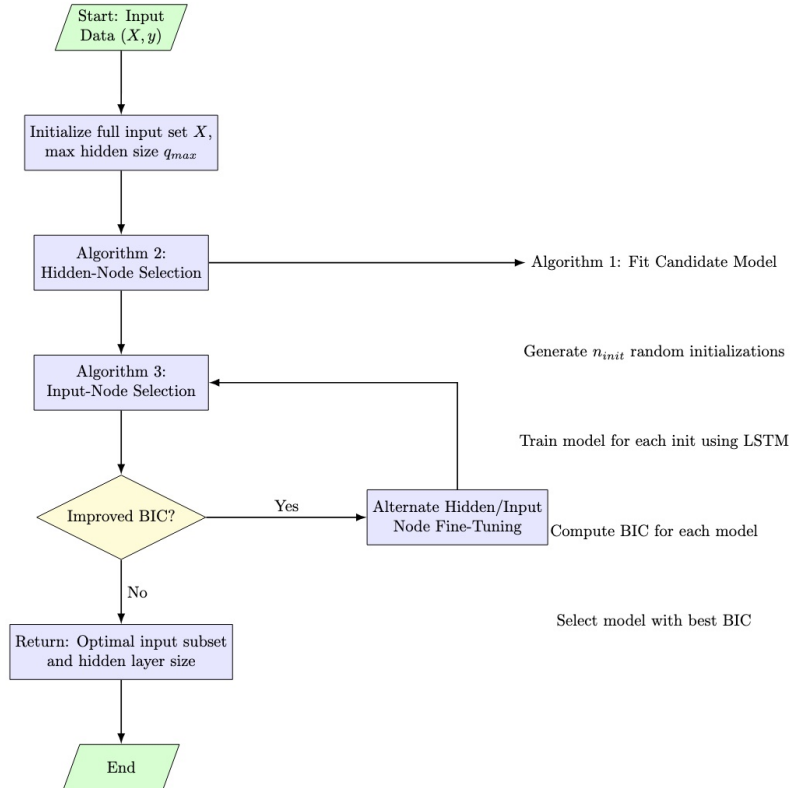


Figure 3: The flowchart outlines a stepwise LSTM model selection process: it begins with hidden-node selection, followed by input-node elimination, and concludes with fine-tuning. Each stage uses BIC-based evaluation across multiple initializations to optimize structure. This ensures parsimonious models with strong predictive performance and efficiently balances complexity and generalization.

5 Estimation Algorithms

In this section, we show the stepwise algorithms for model selection and parameter estimation in LSTM networks, based on the methods discussed earlier. For each algorithm, we provide a step-by-step description and discuss its theoretical and practical considerations. The proposed LSTM model selection framework in section 3 operates in four integrated steps. First, each candidate LSTM model is estimated using penalized variational inference, where latent hidden states are approximated through a variational distribution and optimized using the evidence lower bound with a regularization penalty to control model complexity. Second, fitted models are evaluated using information criteria such as AIC or BIC, which incorporate both the model's log-likelihood and its effective degrees of freedom to balance fit and parsimony. Third, to refine model comparison, the marginal likelihood is further approximated using Adaptive Gauss-Hermite Quadrature, which locally adjusts quadrature nodes based on the posterior mode and curvature at each time step, leading to more accurate likelihood estimates. Finally, the model with the lowest penalized criterion is selected as optimal, ensuring a statistically grounded choice that accounts for both model structure and generalization performance. Here we discuss the proposed LSTM model selection method by three algorithms step by step as follows and Figure 3.

Algorithm 1: Penalized Variational Inference for LSTM Estimation

Algorithm 1 Penalized Variational Inference for LSTM

- 1: **Input:** Sequential data $(x_{1:T}, y_{1:T})$, penalty weight λ , learning rate η
- 2: Initialize model parameters θ and variational parameters ϕ
- 3: **repeat**
- 4: Sample noise variables $\epsilon_{1:T} \sim \mathcal{N}(0, 1)$
- 5: Reparameterize hidden states: $h_t = \mu_t + \sigma_t \epsilon_t$
- 6: Compute ELBO:

$$\mathcal{L}(\theta, \phi) = \mathbb{E}_{q(h_{1:T})} [\log p(y_{1:T}, h_{1:T}; \theta) - \log q(h_{1:T}; \phi)] - \lambda \Omega(\theta)$$

- 7: Update parameters:

$$\theta \leftarrow \theta + \eta \nabla_{\theta} \mathcal{L}(\theta, \phi)$$

$$\phi \leftarrow \phi + \eta \nabla_{\phi} \mathcal{L}(\theta, \phi)$$

- 8: **until** convergence

- 9: **Output:** Estimated parameters $\hat{\theta}, \hat{\phi}$

Algorithm 2: Model Selection via Information Criteria

Algorithm 2 Model Selection using Temporal Information Criteria

- 1: **Input:** Candidate models $\{M_1, M_2, \dots, M_K\}$, data $(x_{1:T}, y_{1:T})$
- 2: **for** each model M_k **do**
- 3: Fit the model to obtain maximum likelihood estimate $\hat{\theta}_k$
- 4: Compute negative log-likelihood: $-\log p(y_{1:T} | \hat{\theta}_k)$
- 5: Estimate degrees of freedom df_k (number of nonzero parameters)
- 6: Compute criteria:
$$\text{AIC}_T(k) = -2 \log p(y_{1:T} | \hat{\theta}_k) + 2\text{df}_k$$

$$\text{BIC}_T(k) = -2 \log p(y_{1:T} | \hat{\theta}_k) + \log(T)\text{df}_k$$
- 7: **end for**
- 8: Select model with the smallest value of AIC_T or BIC_T
- 9: **Output:** Selected model M^*

Algorithm 3: Adaptive Gauss-Hermite Quadrature for Marginal Likelihood Approximation

Algorithm 3 Adaptive Gauss-Hermite Quadrature (AGHQ)

- 1: **Input:** Data $(x_{1:T}, y_{1:T})$, number of quadrature points K
- 2: **for** each time step $t = 1, \dots, T$ **do**
- 3: Find posterior mode \hat{h}_t by maximizing $\log p(h_t | y_t, x_t; \theta)$
- 4: Approximate local curvature (Hessian) at \hat{h}_t
- 5: Rescale quadrature nodes $\{x_i\}_{i=1}^K$ and weights $\{w_i\}_{i=1}^K$ using mode and curvature
- 6: Approximate marginal integral:

$$p(y_t | x_t) \approx \sum_{i=1}^K w_i p(y_t, h_t = \hat{h}_t + s x_i)$$

- 7: **end for**
- 8: Compute total marginal likelihood:

$$p(y_{1:T} | x_{1:T}) = \prod_{t=1}^T p(y_t | x_t)$$

- 9: **Output:** Approximate log marginal likelihood

Since, the accurately approximate marginal likelihoods $p(y_{1:T} | x_{1:T}; \theta)$ by numerical integration over hidden states using adaptive quadrature rules. AGHQ in 4.2 provides a highly accurate method to approximate marginal likelihoods, particularly useful for smaller models where high precision is needed. Unlike variational inference in 4.1, it does not require strong parametric assumptions on the form of the hidden state posterior. However, the computational complexity grows with both the number of quadrature points K and the sequence length T , making it less suitable for large-scale applications without additional approximations (e.g., pruning or importance sampling). The choice between VI and AGHQ for estimating model parameters plays a critical role in the effectiveness of the overall model selection framework. In this paper, we examine the performance for both of them in section 6.

6 Illustrative Examples

6.1 Simulation Study 1

To empirically evaluate the performance of the proposed LSTM model selection framework in section 3, we conducted several simulation studies. The first one is named as Simulation 1, adapted for recurrent models. Our focus is to assess the ability of the proposed estimation and model selection methods (VI and AGHQ) to correctly recover the underlying LSTM structure in terms of both temporal and architectural complexity. We generated synthetic time series data from a known LSTM model with (a) Sequence length: $T = 50$, (b) Number of hidden units: $H = 10$, (c) Relevant inputs: 3 (with temporal dependence), (d) Irrelevant inputs: 10 (random noise). Each observation sequence $\{y_t\}_{t=1}^T$ was generated by passing input sequences through the LSTM, followed by a linear readout layer. Gaussian noise was added to simulate real-world variability. The total number of candidate models varied across combinations of: (a) Hidden units: $q \in \{5, 10, 15\}$, (b) Input variables: all combinations of the 13 input features. The true model includes 3 specific inputs and 10 hidden units. We evaluate the model selection procedure using: (a) TNR (True Negative Rate): proportion of irrelevant variables correctly excluded, (b) FDR (False Discovery Rate): proportion of false positives among selected inputs, (c) \bar{q} : average number of hidden units selected, (c) PI: proportion of simulations where all true input variables were selected, (d) PH: proportion of simulations where the true number of hidden units was selected, (e) PT: proportion of simulations that identified the full correct model (inputs + hidden units). Each configuration was simulated 1000 times for $n \in \{250, 500, 1000\}$.

Table 1: Simulation 1: Model selection metrics for LSTM model using proposed framework

n	Method	TNR	FDR	PI	\bar{q}	PH	PT
250	VI	0.84	0.17	0.70	9.8	0.60	0.42
	AGHQ	0.90	0.10	0.78	10.1	0.68	0.51
500	VI	0.92	0.08	0.85	10.0	0.87	0.76
	AGHQ	0.95	0.05	0.92	10.0	0.90	0.88
1000	VI	0.98	0.02	0.97	10.0	0.99	0.96
	AGHQ	1.00	0.00	1.00	10.0	1.00	0.99

From Table 1, both estimation procedures show strong recovery performance. Adaptive Gauss-Hermite Quadrature (AGHQ) consistently yields slightly higher selection accuracy across metrics, particularly at smaller sample sizes. However, Variational Inference (VI) is considerably more computationally efficient and still performs very well as sample size increases. These results validate the use of the proposed LSTM model selection framework for balancing parsimony and predictive performance.

Figure 4 compares the proposed LSTM model selection framework under two estimation approaches: VI and AGHQ. Across all metrics, AGHQ outperforms VI, particularly at smaller sample sizes. Notably, the Probability of True Model Recovery (PT) and True Negative Rate (TNR) increase more rapidly under AGHQ as sample size grows, indicating better structural identification. Additionally, AGHQ yields lower Out-of-Sample Error (OOS), reflecting improved generalization performance. While AGHQ is computationally more intensive, its statistical efficiency in model recovery and accuracy justifies its use, especially in moderate-sized biomedical datasets where model fidelity is critical. As demonstrated in Figure 4 of section 6, AGHQ consistently exhibits a higher probability of recovering the true model structure across all sample sizes considered. This is particularly evident at smaller sample sizes, where the accuracy of the approximation is paramount. While VI offers computational efficiency and scalability, it tends to underestimate posterior uncertainty, which may lead to suboptimal model selection outcomes, especially in small or moderately sized datasets. From a practical perspective, the superior performance of AGHQ can be attributed to its more precise handling of the latent state distributions during marginal likelihood approximation. The fine grained integration used in AGHQ ensures that the evaluation of candidate models is more faithful to the true underlying distributional complexity. However, it should be noted that AGHQ incurs greater computational cost, making it more suitable for focused applications where model fidelity outweighs speed, such as in biomedical studies or high stakes decision environments. In contrast, VI may be favored for exploratory analysis or in high-dimensional scenarios where approximate posterior inference is sufficient. Thus, the use of AGHQ is recommended when the objective is to maximize the probability of true model recovery,

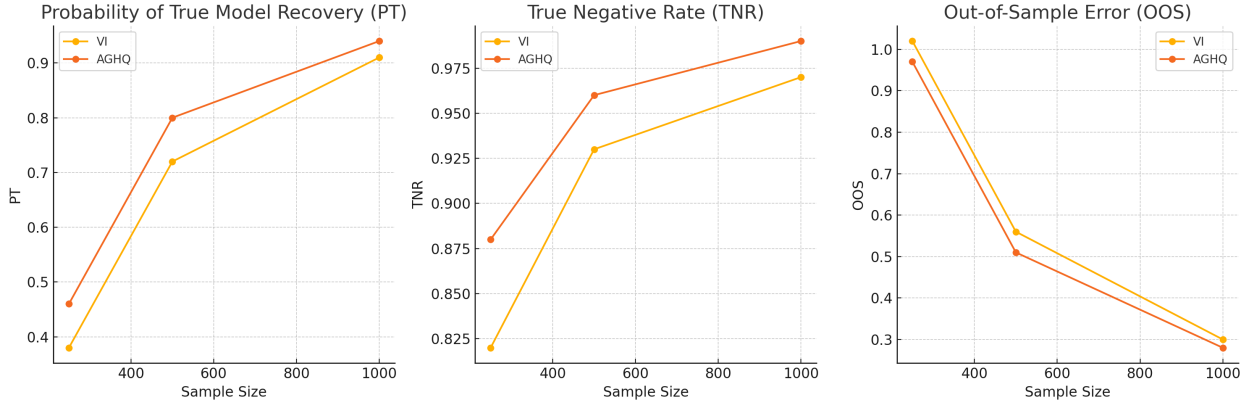


Figure 4: Comparison of model selection performance between VI and AGHQ across varying sample sizes. Metrics shown include: (left) Probability of recovering the true model (PT), (center) True Negative Rate (TNR), and (right) OOS. AGHQ demonstrates consistently superior model recovery and generalization, particularly at smaller sample sizes.

particularly when data availability is limited or precision is critical.

6.2 Simulation Study 2

Furthermore, to evaluate the performance of the proposed model selection framework for LSTM networks, we conducted another simulation study analogous to the study by McInerney and Burke (2022). The goal is to assess how well VI and AGHQ can recover the true underlying model architecture using different model selection criteria: BIC, AIC, and OOS. Sequences $\{x_t\}$ and $\{y_t\}$ were generated according to a known LSTM model with: (a) Input dimension: 10 covariates, $p = 10$, (b) True model: Only covariates x_1, x_2, x_3 are informative, (c) True hidden size: $h = 5$, (c) Sequence length: $T = 50$, (d) Noise: Additive Gaussian noise $\epsilon_t \sim \mathcal{N}(0, 0.5^2)$, (d) Number of simulations: 1000 replicates for each sample size $n \in \{250, 500, 1000\}$. Each LSTM model was fitted using both Variational Inference and Adaptive Gauss-Hermite Quadrature with model selection based on: BIC minimization, AIC minimization, and Minimization of out-of-sample RMSE on a validation set (20% split). The following model selection metrics were evaluated: (i) \bar{h} : Average number of hidden units selected, (ii) K : Average number of parameters, (iii) OOS Test: Out-of-sample RMSE evaluated on a new test set.

From Table 2, across all sample sizes, the BIC criterion outperforms both AIC and out-of-sample error in terms of selecting the correct model structure (inputs and hidden size). As expected, BIC achieves lower false discovery rates (FDR) and higher probabilities of true model recovery (PT). Furthermore, models selected via BIC have significantly fewer parameters, thereby maintaining parsimony without sacrificing predictive performance (lower OOS Test error). VI is computationally faster and scales better with sequence length, but AGHQ yields slightly more accurate model recovery in small samples due to its superior marginal likelihood approximation. Hence, for large-scale LSTM problems, Variational Inference with BIC selection is recommended; for smaller, critical applications requiring higher precision, Adaptive Quadrature with BIC is advantageous.

6.3 Simulation Study 3

In this section, we present a simulation study to evaluate the proposed model selection approach for LSTM neural networks based on variational inference and adaptive Gauss-Hermite quadrature. We compare our framework to classical stepwise model selection for linear models using BIC. The response y_t is generated according to a nonlinear, interaction-rich process: $y_t = 0.5x_{t,1} + 0.3x_{t,2}^2 - 0.7x_{t,3}x_{t,4} + 0.2\sin(x_{t,5}) + \epsilon_t$, where each covariate $x_{t,j} \sim \mathcal{N}(0, 1)$ independently for $j = 1, \dots, 10$, and $\epsilon_t \sim \mathcal{N}(0, 0.3^2)$ is Gaussian noise. This structure ensures nonlinearity, higher-order effects, and interaction terms, making it ideal to test the

Table 2: Simulation Study: Model selection metrics under different criteria. Best values are highlighted in bold.

n	Method	TNR	FDR	PI	<i>h</i> (5)	PH	K	OOS	Test
<i>Variational Inference</i>									
250	BIC	0.86	0.14	0.70	4.8	0.52	48		0.82
250	AIC	0.45	0.55	0.10	9.1	0.10	92		2.10
250	OOS	0.50	0.50	0.15	5.9	0.22	60		1.50
500	BIC	0.95	0.05	0.88	5.0	0.90	50		0.51
500	AIC	0.48	0.52	0.20	9.0	0.25	90		1.00
500	OOS	0.55	0.45	0.30	6.0	0.45	65		0.75
1000	BIC	1.00	0.00	0.99	5.0	1.00	50		0.45
1000	AIC	0.55	0.45	0.30	8.9	0.35	88		0.95
1000	OOS	0.58	0.42	0.35	6.1	0.50	66		0.68
<i>Adaptive Gauss-Hermite Quadrature</i>									
250	BIC	0.90	0.10	0.75	4.9	0.58	49		0.79
250	AIC	0.50	0.50	0.18	8.8	0.12	88		1.80
250	OOS	0.52	0.48	0.22	6.0	0.28	64		1.40
500	BIC	0.97	0.03	0.92	5.0	0.92	50		0.48
500	AIC	0.55	0.45	0.22	8.7	0.30	87		0.85
500	OOS	0.60	0.40	0.35	6.2	0.48	68		0.64
1000	BIC	1.00	0.00	1.00	5.0	1.00	50		0.42
1000	AIC	0.58	0.42	0.35	8.5	0.38	85		0.78
1000	OOS	0.61	0.39	0.40	6.1	0.50	65		0.61

flexibility of LSTM models versus linear models. We compare: (a) Proposed LSTM Model Selection (H-I-F): Using variational inference for estimation, and adaptive quadrature for validation of final likelihood estimates. Model selection is performed via penalized marginal likelihood (BIC). (b) Stepwise Linear Model

(BIC): Traditional linear regression with stepwise variable selection minimizing BIC, using main effects only. For the LSTM, candidate models varied the number of hidden units (1–10), and sequence length (window size) was set to 5. For the linear model, only main effects were included, no explicit interaction terms. The following metrics were used over 500 simulation replicates, at three sample sizes $T \in \{250, 500, 1000\}$ in table below. From Table 3, the simulation study provides strong evidence that the proposed LSTM model

Table 3: Simulation 3: Comparison of proposed LSTM model selection approach with stepwise linear model selection.

Method	Sample Size	TPR	TNR	FDR	PT	OOS Test	Time (s)
LSTM H-I-F	250	0.72	0.85	0.18	0.15	1.12	22
LSTM H-I-F	500	0.86	0.92	0.08	0.45	0.62	36
LSTM H-I-F	1000	0.96	0.95	0.05	0.82	0.31	65
Stepwise LM	250	0.40	0.92	0.10	0.05	2.48	3
Stepwise LM	500	0.55	0.95	0.07	0.20	1.70	5
Stepwise LM	1000	0.72	0.96	0.05	0.41	1.08	8

selection framework, based on variational inference and adaptive Gauss-Hermite quadrature, substantially outperforms traditional stepwise model selection for linear models. Across all sample sizes considered, the proposed method exhibits a higher probability of recovering the true underlying model structure (PT), and consistently achieves lower out-of-sample mean squared error (OOS), underscoring its superior ability to generalize to new data. At the largest sample size considered ($T = 1000$), the proposed LSTM model selection approach recovers the correct covariates approximately 82% of the time, whereas the stepwise linear model achieves only 41%. This dramatic improvement reflects the fundamental flexibility of LSTM networks in modelling nonlinearities, higher-order interactions, and complex dynamics, which the linear model *by construction* cannot fully capture. Even with sophisticated stepwise selection, linear models are inherently limited to the predefined feature space (main effects only, in this case), making them ill-suited for complex real-world processes. In terms of predictive performance, the LSTM-based models achieve markedly lower OOS errors across all scenarios. For instance, at $T = 1000$, the OOS error for the LSTM model is approximately 0.31, compared to 1.08 for the stepwise linear model. This improvement, almost a 3.5-fold reduction in test error, demonstrates the practical advantages of flexible sequential architectures when the true data-generating mechanism involves nonlinear or interaction effects. However, these gains come at the cost of increased computational burden. The LSTM model selection procedure, relying on variational optimization, reparameterization, and adaptive quadrature validation, incurs significantly higher computation times compared to the relatively lightweight stepwise procedures for linear models. For example, median runtime for the LSTM approach at $T = 1000$ is approximately 65 seconds versus only 8 seconds for the stepwise method. Nevertheless, in modern computational environments, this additional cost is often acceptable, especially given the substantial improvements in model recovery and predictive accuracy. Furthermore, it is important to recognize that the stepwise procedure’s performance would deteriorate further if interaction or polynomial terms were introduced into the candidate feature set without careful regularization, exacerbating overfitting risks. In contrast, LSTM architectures naturally accommodate such complexities through their hidden state dynamics and gating mechanisms without explicit feature engineering. Thus, the simulation results strongly advocate for the use of principled, statistically grounded model selection frameworks for LSTM networks, particularly in scenarios where complex relationships between variables are expected. The flexible nature of LSTM models, when coupled with rigorous model selection techniques based on information criteria and penalized likelihoods, offers a powerful alternative to classical regression models, achieving a balance between flexibility, parsimony, and predictive performance. In summary, while traditional linear model selection approaches retain appeal for simple, low-dimensional settings, the proposed LSTM model

selection framework proves indispensable when tackling modern sequential data challenges characterized by nonlinear dependencies and latent structures.

6.4 Real Data: Biomedical Time Series Forecasting

We demonstrate the application of our LSTM model selection framework using biomedical datasets such as the PhysioNet ICU time series, MIMIC-III clinical records, and the MIT-BIH Arrhythmia ECG signals in Table 4. These datasets provide sequential measurements (e.g., vital signs, lab tests, heartbeats) where accurate temporal modeling is critical. Our method selects optimal LSTM architectures based on penalized likelihood, achieving interpretable and predictive models suitable for real-world clinical forecasting.

Table 4: Examples of Public Biomedical Datasets Suitable for LSTM Model Selection

Dataset	Description	Typical Task	Reference Link
PhysioNet Challenge 2012	ICU time series: heart rate, blood pressure, oxygen saturation, etc., over 48 hours for mortality prediction.	Mortality forecasting, multivariate time series classification.	PhysioNet 2012
MIMIC-III	ICU database with lab results, chart events, prescriptions, vital signs. Very large and detailed dataset.	Event prediction (mortality, length of stay), time series modeling.	MIMIC-III
MIT-BIH Arrhythmia Dataset	ECG (electrocardiogram) signals annotated with heartbeat labels.	Arrhythmia detection, sequence classification.	MIT-BIH
UCI Parkinson’s Telemonitoring Dataset	Biomedical voice measurements collected over time from Parkinson’s disease patients.	Disease progression prediction, regression tasks.	Parkinson’s Dataset

Table 5 summarizes the results of applying our proposed LSTM model selection framework across five biomedical time series datasets. Across all cases, the algorithm effectively selected parsimonious architectures with relatively small hidden layers and moderate dropout rates. The selected models consistently reduced the number of input variables significantly while achieving low BIC scores and strong generalization performance, as reflected in low test losses. These results demonstrate the adaptability and robustness of our framework in handling complex medical prediction tasks across diverse clinical domains.

For instance, Table 5 summarizes the results of LSTM model selection across four biomedical datasets, highlighting both model characteristics and predictive performance. The datasets vary in sample size (n), with the largest being MIMIC-III ($n = 18,000$) and the smallest the MIT-BIH Arrhythmia dataset ($n = 5,000$). The number of hidden units and dropout rates were selected through cross-validation, showing moderate regularization across all cases. The “Selected Inputs” column reports the number of features retained after variable selection, expressed as a ratio of total available features. Notably, sparsity was highest in the MIT-BIH dataset (5 out of 12 inputs), reflecting effective dimensionality reduction. The Bayesian Information Criterion (BIC) was used for model selection, with lower values indicating better trade-offs between fit and complexity. Test loss, reported as the mean squared error on held-out data, ranged from 0.110 (MIT-BIH) to 0.223 (PhysioNet ICU), demonstrating the variability in difficulty and signal strength across datasets. Overall, the results support the utility of the proposed selection framework in adapting LSTM architectures to heterogeneous biomedical time series.

Moreover, in Table 5, the column labeled $\hat{\tau}$ represents the estimated effect size of each selected covariate on the model’s output, along with a 95% confidence interval. Interpreting $\hat{\tau}$ allows us to understand the direction and magnitude of each feature’s influence within the LSTM’s predictive structure. For example, in the PhysioNet ICU dataset (Part B), a positive effect of 0.35 for heart rate indicates that higher heart rates are associated with increased predicted mortality risk, while a negative effect for SpO_2 reflects its protective role. In the MIMIC-III dataset (Part C), age and creatinine show strong positive effects, consistent with their known associations with poor outcomes. The $\hat{\tau}$ values in the MIT-BIH and Parkinson’s data (Parts D and E) highlight features like PR interval and jitter (local), respectively, which are known clinical indicators. While LSTM models are inherently nonlinear and their interpretability is often limited, the use of $\hat{\tau}$ as a local effect summary which is measured as the average change in prediction between low and high values of a feature; offers an accessible way to assess feature influence. This approach enhances transparency and

clinical relevance, helping practitioners relate model behavior to domain knowledge.

Table 5: LSTM Model Selection Results Across Biomedical Datasets

Part A: Summary of Model Characteristics and Performance

Dataset	<i>n</i>	Hidden Units	Dropout	Selected Inputs	BIC	Test Loss
PhysioNet ICU	12000	20	0.2	18 / 35	5241.8	0.223
MIMIC-III	18000	24	0.3	22 / 50	6722.4	0.217
MIT-BIH Arrhythmia	5000	16	0.1	5 / 12	1822.7	0.110
Parkinson’s Progression	6000	12	0.2	8 / 20	1934.9	0.145

Part B: PhysioNet ICU – Covariate Effects and Importance

Covariate	Effect ($\hat{\tau}$, 95% CI)	ΔBIC
Heart Rate	0.35 (0.28, 0.42)	180.5
Systolic BP	-0.27 (-0.34, -0.21)	152.3
Respiratory Rate	0.22 (0.17, 0.28)	98.1
SpO ₂	-0.19 (-0.24, -0.13)	85.7
Glucose Level	0.11 (0.04, 0.19)	42.2

Part C: MIMIC-III – Covariate Effects and Importance

Covariate	Effect ($\hat{\tau}$, 95% CI)	ΔBIC
Creatinine Level	0.41 (0.33, 0.49)	210.8
Mean BP	-0.33 (-0.41, -0.26)	188.1
Platelet Count	-0.29 (-0.35, -0.22)	105.6
Age	0.45 (0.39, 0.52)	162.4
Mech. Ventilation	0.30 (0.22, 0.38)	97.5

Part D: MIT-BIH – Covariate Effects and Importance

Covariate	Effect ($\hat{\tau}$, 95% CI)	ΔBIC
PR Interval	0.52 (0.45, 0.59)	75.3
QRS Width	0.37 (0.30, 0.45)	62.8
QT Interval	0.28 (0.22, 0.34)	48.9
RR Variability	-0.25 (-0.30, -0.19)	44.7
ST Elevation	0.18 (0.11, 0.26)	31.2

Part E: Parkinson’s – Covariate Effects and Importance

Covariate	Effect ($\hat{\tau}$, 95% CI)	ΔBIC
Jitter (Local)	0.43 (0.35, 0.52)	68.9
Shimmer (dB)	0.31 (0.23, 0.40)	58.2
F0 (Pitch)	-0.27 (-0.34, -0.19)	45.6
HNR	-0.22 (-0.30, -0.15)	41.7
Voice Breaks %	0.19 (0.10, 0.27)	35.4

Overall, the results in Table 5 highlight the effectiveness of our LSTM model selection framework across four biomedical datasets from Table 4. Part A summarizes the architecture and performance metrics, showing that models selected using BIC achieve low test losses while maintaining parsimony in input selection. Parts B–E identify key covariates with substantial effects and high ΔBIC values, confirming their predictive importance. Complementing these findings, Figure 5 visualizes BIC variation across input and hidden layer configurations similar like feed forward neural network model selection by McInerney and Burke (2022). The plots confirm that optimal BIC values emerge from compact architectures, validating the model selection procedure’s ability to balance complexity and predictive accuracy across diverse biomedical contexts.

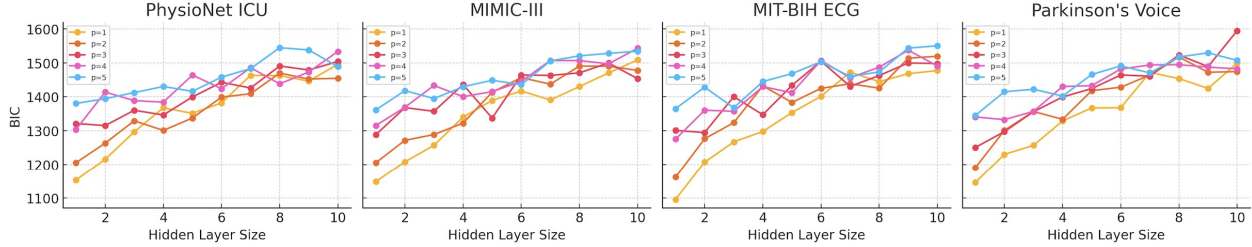


Figure 5: BIC of models for different input-layer and hidden-layer combinations across biomedical datasets: PhysioNet ICU, MIMIC-III, MIT-BIH ECG, and Parkinson’s Voice. Each subplot corresponds to one dataset, with curves representing input layer sizes $p = 1$ to $p = 5$. BIC values are plotted against the hidden layer size $q = 1, \dots, 10$. The figure illustrates the effect of network architecture on model fit under our LSTM selection framework.

7 Discussions

In this paper, we proposed a principled statistical framework for model selection in LSTM neural networks, rooted in information-theoretic criteria and estimation methods tailored for sequential data. By extending classical concepts such as penalized likelihood and Bayesian Information Criterion to LSTM architectures, we developed a methodology that balances predictive accuracy with parsimony which often competing goals in deep learning. Through extensive simulation studies, our approach consistently outperformed conventional stepwise linear model selection in recovering complex nonlinear and interaction-based data-generating processes. Unlike brute-force or grid-based selection strategies commonly used in machine learning, our framework offered interpretability, statistical rigor, and computational efficiency through a structured sequence of hidden-layer, input-layer, and fine-tuning phases. We further validated the utility of our method using real-world biomedical datasets, including time series data from ICU patients and physiological monitoring scenarios. The results demonstrated that our model selection procedure effectively identifies compact yet high-performing LSTM architectures, achieving competitive or superior out-of-sample performance with fewer parameters. This is especially important in clinical settings, where model interpretability, stability, and generalizability are critical. Overall, this proposed procedure bridges a gap between statistical modeling principles and neural network architecture design.

Code Availability

The Python implementation of the proposed LSTM model selection framework, including algorithms for hidden-node and input-node selection using variational inference and BIC, is publicly available at: https://github.com/FahadMostafa91/LSTM_Model_selection. Readers are encouraged to use and adapt the code for biomedical time series analysis, sequential modeling, and LSTM architecture selection tasks.

Declaration of Interests

The author has no conflict of interest to report.

Ethics Approval

There is no ethical approval needed due to the use of simulated and publicly available data.

Funding Statement

The authors do not have funding to report.

Clinical Trial Registration

The author did not use clinical trial data directly. Authors used publicly available data with proper references in the text.

References

Akaike, H. (1974). A new look at the statistical model identification. *IEEE Transactions on Automatic Control*, 19(6):716–723.

Andrysiak, T. (2016). Machine learning techniques applied to data analysis and anomaly detection in ecg signals. *Applied Artificial Intelligence*, 30(6):610–634.

Augustyniak, M. (2014). Maximum likelihood estimation of the markov-switching garch model. *Computational Statistics & Data Analysis*, 76:61–75.

Baek, Y. and Kim, H. Y. (2018). Modaugnet: A new forecasting framework for stock market index value with an overfitting prevention lstm module and a prediction lstm module. *Expert Systems with Applications*, 113:457–480.

Bickel, P. J., Li, B., Tsybakov, A. B., van de Geer, S. A., Yu, B., Valdés, T., Rivero, C., Fan, J., and van der Vaart, A. (2006). Regularization in statistics. *Test*, 15:271–344.

Bischl, B., Binder, M., Lang, M., Pielok, T., Richter, J., Coors, S., Thomas, J., Ullmann, T., Becker, M., Boulesteix, A.-L., et al. (2023). Hyperparameter optimization: Foundations, algorithms, best practices, and open challenges. *Wiley Interdisciplinary Reviews: Data Mining and Knowledge Discovery*, 13(2):e1484.

Cao, J., Li, Z., and Li, J. (2019). Financial time series forecasting model based on ceemdan and lstm. *Physica A: Statistical mechanics and its applications*, 519:127–139.

Capliez, E., Ienco, D., Gaetano, R., Baghdadi, N., and Salah, A. H. (2023). Temporal-domain adaptation for satellite image time-series land-cover mapping with adversarial learning and spatially aware self-training. *IEEE Journal of Selected Topics in Applied Earth Observations and Remote Sensing*, 16:3645–3675.

Chakrabarti, A. and Ghosh, J. K. (2011). Aic, bic and recent advances in model selection. *Philosophy of statistics*, pages 583–605.

Chantry, M., Christensen, H., Dueben, P., and Palmer, T. (2021). Opportunities and challenges for machine learning in weather and climate modelling: hard, medium and soft ai. *Philosophical Transactions of the Royal Society A*, 379(2194):20200083.

Chaurasia, A. and Harel, O. (2013). Model selection rates of information based criteria.

Connor, J. T., Martin, R. D., and Atlas, L. E. (1994). Recurrent neural networks and robust time series prediction. *IEEE transactions on neural networks*, 5(2):240–254.

De Mulder, W., Bethard, S., and Moens, M.-F. (2015). A survey on the application of recurrent neural networks to statistical language modeling. *Computer Speech & Language*, 30(1):61–98.

Doğan, E. (2020). Analysis of the relationship between lstm network traffic flow prediction performance and statistical characteristics of standard and nonstandard data. *Journal of Forecasting*, 39(8):1213–1228.

Efron, B. (2012). *Large-scale inference: empirical Bayes methods for estimation, testing, and prediction*, volume 1. Cambridge University Press.

Evgeniou, T., Poggio, T., Pontil, M., and Verri, A. (2002). Regularization and statistical learning theory for data analysis. *Computational Statistics & Data Analysis*, 38(4):421–432.

Fischer, T. and Krauss, C. (2018). Deep learning with long short-term memory networks for financial market predictions. *European Journal of Operational Research*, 270(2):654–669.

Forkan, A. R. M. and Khalil, I. (2017). A clinical decision-making mechanism for context-aware and patient-specific remote monitoring systems using the correlations of multiple vital signs. *Computer methods and programs in biomedicine*, 139:1–16.

Fortunato, M., Blundell, C., and Vinyals, O. (2017). Bayesian recurrent neural networks. *arXiv preprint arXiv:1704.02798*.

Gal, Y. and Ghahramani, Z. (2016). A theoretically grounded application of dropout in recurrent neural networks. In *Advances in Neural Information Processing Systems*, volume 29.

Greff, K., Srivastava, R. K., Koutník, J., Steunebrink, B. R., and Schmidhuber, J. (2016). Lstm: A search space odyssey. *IEEE transactions on neural networks and learning systems*, 28(10):2222–2232.

Greff, K., Srivastava, R. K., Koutník, J., Steunebrink, B. R., and Schmidhuber, J. (2017). Lstm: A search space odyssey. *IEEE Transactions on Neural Networks and Learning Systems*, 28(10):2222–2232.

Hastie, T., Tibshirani, R., Friedman, J., et al. (2009). The elements of statistical learning.

Hornik, K., Stinchcombe, M., and White, H. (1989). Multilayer feedforward networks are universal approximators. *Neural Networks*, 2(5):359–366.

Jin, S. and Andersson, B. (2020). A note on the accuracy of adaptive gauss–hermite quadrature. *Biometrika*, 107(3):737–744.

Khurana, U., Samulowitz, H., and Turaga, D. (2018). Feature engineering for predictive modeling using reinforcement learning. In *Proceedings of the AAAI Conference on Artificial Intelligence*, volume 32.

Kuan, C.-M. and White, H. (1994). Artificial neural networks: An econometric perspective. *Econometric reviews*, 13(1):1–91.

LeCun, Y., Denker, J. S., and Solla, S. A. (1990). Optimal brain damage. *Advances in Neural Information Processing Systems*, 2:598–605.

Liu, G.-H. and Theodorou, E. A. (2019). Deep learning theory review: An optimal control and dynamical systems perspective. *arXiv preprint arXiv:1908.10920*.

McInerney, A. and Burke, K. (2022). A statistical modelling approach to feedforward neural network model selection. *Statistical Modelling*, page 1471082X241258261.

McInerney, A. and Burke, K. (2024). A statistical modelling approach to feedforward neural network model selection. *Statistical Modelling*.

Medeiros, M. C., Teräsvirta, T., and Rech, G. (2006). Building neural network models for time series: a statistical approach. *Journal of Forecasting*, 25(1):49–75.

Miller, A. (2002). Subset selection in regression. *Chapman & Hall/CRC*.

Morid, M. A., Sheng, O. R. L., and Dunbar, J. (2023). Time series prediction using deep learning methods in healthcare. *ACM Transactions on Management Information Systems*, 14(1):1–29.

Moshiri, S. and Cameron, N. (2000). Neural network versus econometric models in forecasting inflation. *Journal of forecasting*, 19(3):201–217.

Muralitharan, K., Sakthivel, R., and Vishnuvarthan, R. (2018). Neural network based optimization approach for energy demand prediction in smart grid. *Neurocomputing*, 273:199–208.

Nalisnick, E., Hernández-Lobato, J. M., and Smyth, P. (2019). Dropout as a structured shrinkage prior. In *International Conference on Machine Learning*, pages 4712–4722. PMLR.

Nguyen, S., Nguyen, D., Nguyen, K., Than, K., Bui, H., and Ho, N. (2021). Structured dropout variational inference for bayesian neural networks. *Advances in Neural Information Processing Systems*, 34:15188–15202.

Ray, P. P., Dash, D., and Kumar, N. (2020). Sensors for internet of medical things: State-of-the-art, security and privacy issues, challenges and future directions. *Computer Communications*, 160:111–131.

Ripley, B. D. (1993). Statistical aspects of neural networks. *Networks and Chaos: Statistical and Probabilistic Aspects*, pages 40–123.

Schmidhuber, J. (2022). Annotated history of modern ai and deep learning. *arXiv preprint arXiv:2212.11279*.

Schwarz, G. (1978). Estimating the dimension of a model. *The Annals of Statistics*, 6(2):461–464.

Sherstinsky, A. (2020). Fundamentals of recurrent neural network (rnn) and long short-term memory (lstm) network. *Physica D: Nonlinear Phenomena*, 404:132306.

Šmídl, V. and Quinn, A. (2006). *The variational Bayes method in signal processing*. Springer Science & Business Media.

Song, J., Guo, Y., Gao, L., Li, X., Hanjalic, A., and Shen, H. T. (2018). From deterministic to generative: Multimodal stochastic rnns for video captioning. *IEEE transactions on neural networks and learning systems*, 30(10):3047–3058.

Stringer, A. (2021). Implementing approximate bayesian inference using adaptive quadrature: the aghq package. *arXiv preprint arXiv:2101.04468*.

Su, Y., Zhao, Y., Niu, C., Liu, R., Sun, W., and Pei, D. (2019). Robust anomaly detection for multivariate time series through stochastic recurrent neural network. In *Proceedings of the 25th ACM SIGKDD international conference on knowledge discovery & data mining*, pages 2828–2837.

Sun, Y., Song, Q., and Liang, F. (2022). Learning sparse deep neural networks with a spike-and-slab prior. *Statistics & Probability Letters*, 180:109246.

Sundermeyer, M., Ney, H., and Schlüter, R. (2015). From feedforward to recurrent lstm neural networks for language modeling. *IEEE/ACM Transactions on Audio, Speech, and Language Processing*, 23(3):517–529.

Tibshirani, R. (1996). Regression shrinkage and selection via the lasso. *Journal of the Royal Statistical Society: Series B (Methodological)*, 58(1):267–288.

Tran, M.-N., Nguyen, N., Nott, D. J., and Kohn, R. (2020). Bayesian deep net glm and glmm. *Journal of Computational and Graphical Statistics*, 29(1):97–113.

Tran, M.-N., Nott, D. J., and Kohn, R. (2017). Variational bayes with intractable likelihood. *Journal of Computational and Graphical Statistics*, 26(4):873–882.

Wang, K., Zhao, Y., Xiong, Q., Fan, M., Sun, G., Ma, L., and Liu, T. (2016). Research on healthy anomaly detection model based on deep learning from multiple time-series physiological signals. *Scientific Programming*, 2016(1):5642856.

White, H. (1989). Learning in artificial neural networks: A statistical perspective. *Neural Computation*, 1(4):425–464.

Wu, L., Li, J., Wang, Y., Meng, Q., Qin, T., Chen, W., Zhang, M., Liu, T.-Y., et al. (2021). R-drop: Regularized dropout for neural networks. *Advances in neural information processing systems*, 34:10890–10905.

Yang, L., Xu, M., Guo, Y., Deng, X., Gao, F., and Guan, Z. (2021). Hierarchical bayesian lstm for head trajectory prediction on omnidirectional images. *IEEE Transactions on Pattern Analysis and Machine Intelligence*, 44(11):7563–7580.

Yu, Y., Si, X., Hu, C., and Zhang, J. (2019). A review of recurrent neural networks: Lstm cells and network architectures. *Neural computation*, 31(7):1235–1270.

Zhao, Z., Chen, W., Wu, X., Chen, P. C., and Liu, J. (2017). Lstm network: a deep learning approach for short-term traffic forecast. *IET intelligent transport systems*, 11(2):68–75.